Available online at www.sciencedirect.com
ScienceDirect
Journal of Nuclear Materials 374 (2008) 431–436
journal of nuclear materials
www.elsevier.com/locate/jnucmat

Two-step two-stage fission gas release model

Yong-soo Kim [a,*], Chan-bock Lee [b]

[a] Nuclear Engineering Department, Hanyang University, 17 Haengdang-Dong, Seoul 133-791, Republic of Korea
[b] KAERI (Korea Atomic Energy Research Institute), 150 Deokjin-Dong, Taejon 305-353, Republic of Korea

Received 25 June 2007; accepted 1 October 2007

Abstract

A two-step two-stage model is developed in this study on the basis of the recent theoretical model. This model incorporates a two-step burn-up factor in the two-stage diffusion processes in the grain lattice and at the grain boundary during the fission gas release. In-pile data sets available in FRAPCON-3 code are used to validate the model. Results show that the predictions are in better agreement with the experimental measurements than those of any other models built in the code over the entire burn-up range up to 75000 MWd/MTU.

PACS: 28.41.Ak; 61.72.Mm; 66.30.Jt

1. Introduction

Since the operation mode of light water reactors (LWRs) changed from annual to extended/high burn-up fuel cycle in the late 1980s, attention has focused on fission gas release phenomena [1–7]. Many studies have reported that the fractional fission gas release is augmented with increasing burn-up, especially in the high burn-up regime. It is now generally accepted that fission gas release can be a potential design-limiting factor in the high performance fuel development because it plays a crucial role in the thermo-mechanical behavior of current LWR fuel rods under heavy duty operation.

In fact, uranium dioxide fuel is a polycrystalline ceramic material consisting of many small grains. Because of the high operating temperature, fission gas atoms generated by fission reactions inside the fuel grain lattice begin to volumetrically diffuse onto the grain boundaries, and on reaching these, continuously diffuse along the grain boundaries until they are released into the open space in the fuel rod. Thus, the grain boundaries are believed to play a significant role in the release process, as do inter- and intra-fission gas bubbles in the high burn-up fuels. Excellent works on the effects of the grain boundaries have been reported by several authors [8–13]. Nevertheless, analytical approaches on the two-stage fission gas transport have not been successful, and thus, the role of the grain boundaries and related phenomena is not yet clearly understood.

Since the early work done by Booth [14], in which fuel is treated as an assembly of uniform spheres with a perfect sink boundary condition, the accumulation of in-pile experience has revealed that fission gas–gas interactions during the diffusion process lead to the formation of gas-filled intra-granular bubbles, especially in the increased fuel burn-up. In addition, the assumption of the perfect sink does not conform to the micro-graphical observations that gas atoms accumulate continuously at the grain boundaries, which mostly cause the formation of inter-granular bubbles. It has been also found that fission fragments can resolve these bubbles into the fuel grain matrix or to the near-grain boundary region while both inter- and intra-gas bubbles trap the diffusing fission gas atoms. The diffusion process of the fission gas atoms with the intra- and inter-granular bubbles in a high burn-up fuel is shown schematically in Fig. 1.

In actuality, the precipitation of gas atoms in the bubbles and their resolution into the lattice complicate the

* Corresponding author. Tel.: +82 2 2220 0467; fax: +82 2 2281 5131.
E-mail address: yongskim@hanyang.ac.kr (Y.-s. Kim).

0022-3115/$ - see front matter
doi:10.1016/j.jnucmat.2007.10.002

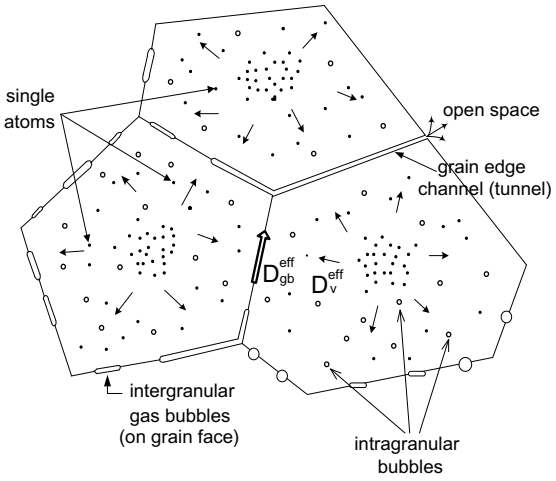

Fig. 1. A schematic diagram of the two principal diffusion processes with effective diffusion coefficients of D_v^{eff} and D_{gb}^{eff}, respectively.

analysis of the fission gas release phenomenon. Thus, several mechanistic models have been proposed with a non-zero grain boundary concentration [15–18]. Speight proposed a method to determine the grain boundary concentration [15], and Turnbull derived an analytical solution for the non-zero constant boundary concentration case [16]. Forsberg and Massih considered a time-dependent grain boundary condition and treated it numerically by assuming that the fission gas atoms are released completely when the grain boundary concentration exceeds a certain threshold value [18].

Recently a theoretical two-stage model was proposed that mechanistically describes the diffusion processes of the fission gas atoms in the two separate regions: grain lattice and grain boundary [19]. The model sets up two exact simultaneous partial differential equations for the fission

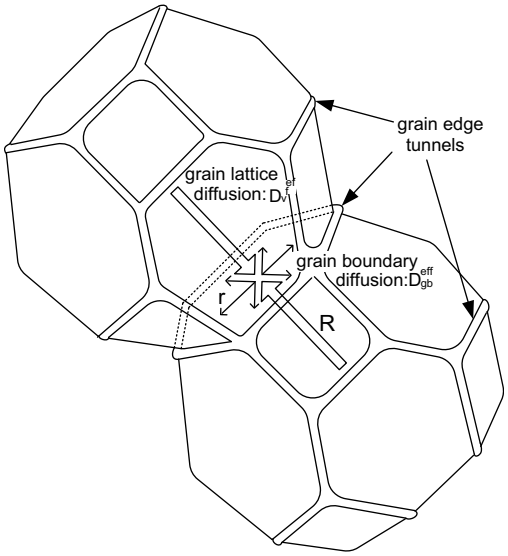

Fig. 2. Effective grain lattice and grain boundary diffusion processes assumed in the two-stage model.

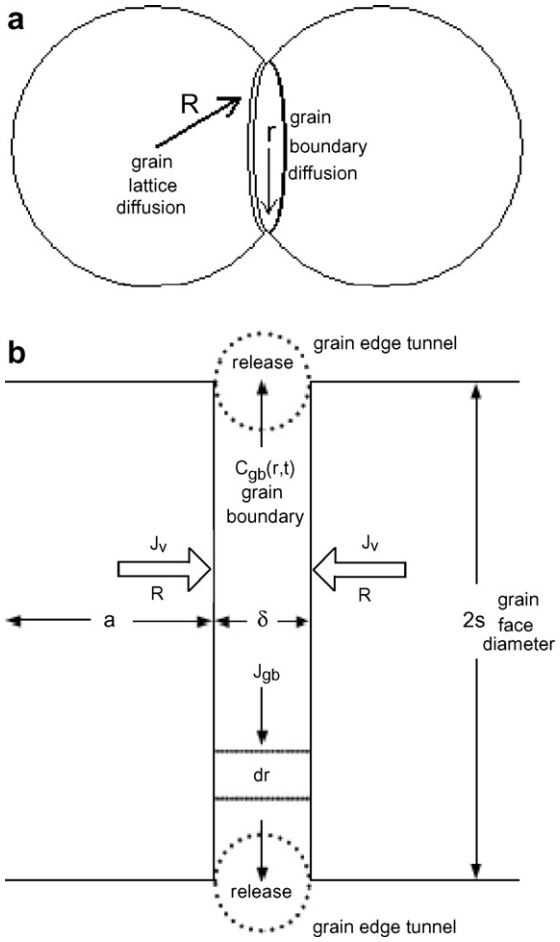

Fig. 3. (a) A schematic diagram of two contacting equivalent spheres. (b) Concentration balance of fission gas atoms within the grain boundary.

gas atom concentrations in the grain lattice and at the grain boundary with the appropriate time-dependent boundary conditions. Then, with the incorporation of the relative diffusivity ratio, α, defined as D_v^{eff}/D_{gb}^{eff}, the model successfully explains the role and the effect of the grain boundaries in fission gas release behavior (Figs. 2 and 3).

In this study, this model is expanded to a two-step two-stage model in which the two-stage diffusion process is coupled with a two-step burn-up factor. The stepwise burn-up factor reflects recent in-pile experiences (Fig. 4) that the fractional fission gas release is rapidly augmented with increasing fuel burn-up, especially in the high burn-up regime, which is primarily due to the strong inter-linkage of the inter-granular fission gas bubbles [20].

2. Development of the model

2.1. Two-stage model

In the two-stage model, fission gas transport is broken down into two principal processes: grain lattice diffusion and grain boundary diffusion, coupled with the bubble trap and resolution [19]. This coupling leads to the definitions of

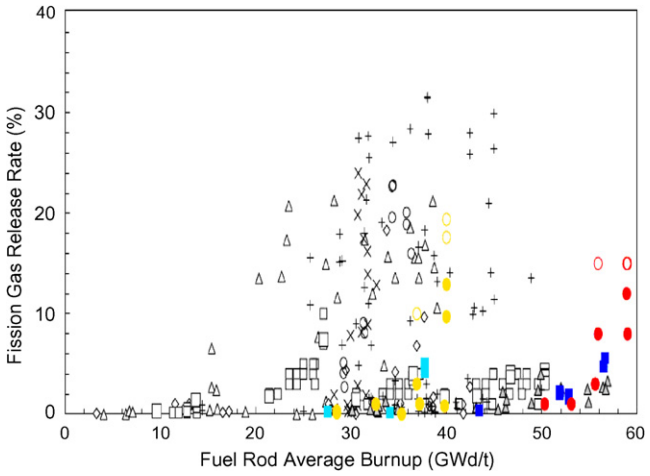

Fig. 4. Compiled in-pile data on the fractional fission gas release [20].

effective grain lattice diffusion, $D_v^{eff} = \left(\frac{b}{b+g}\right)D_v$, and effective grain boundary diffusion, $D_{gb}^{eff} = \left(\frac{b}{b+g}\right)D_{gb}$, respectively, as originally defined by Speight [15]. Fig. 2 shows a schematic drawing of the fundamental processes of the model, assuming that a grain has an ideal tetrakaidecahedral structure, and that the fission gas bubbles at the grain edges are linked together to form grain edge tunnels that are connected to the open space inside the fuel rod. This means that, after the fission gas atoms generated inside grain lattice diffuse volumetrically through the grain lattice and reach the grain boundaries, they surface-diffuse again through the grain boundaries and release eventually into the open space, on arriving at the grain edge tunnels. In actuality, this provides the basis of cylindrical geometric approach to solve the following solute transport formulation in the grain boundary.

In this analysis, the polyhedral grain is treated as an equivalent sphere. Fig. 3(a) and (b) shows a schematic drawing of the two contacting equivalent spheres which form a flat surface of grain boundary and the concentration balance of the solute atoms in the grain boundary, respectively.

Therefore, the governing equation for the effective grain lattice diffusion in the sphere can be formulated in the following way:

$$\frac{\partial C_v}{\partial t} = \beta + \frac{1}{R^2}\frac{\partial}{\partial R}\left(D_v^{eff} R^2 \frac{\partial C_v}{\partial R}\right) \tag{1}$$

with the initial condition of $C_v(R,0) = 0$, and the boundary conditions of $C_v(0,t) =$ finite and $C_v(a,t) = \overline{C}_{gb}(t)$. In Eq. (1), C_v is the volumetric fission gas concentration within the grain, β is the fission gas generation rate, and a is the equivalent radius of the grain. The lattice diffusion term in the RHS of Eq. (1) is expressed in spherical coordinates since the solute atoms are assumed to diffuse onto the surface of the equivalent sphere, as seen in Fig. 3(a). Note that the surface boundary condition is the time-dependent average grain boundary concentration, $\overline{C}_{gb}(t)$, which needs to be determined simultaneously.

Meanwhile, the fission gas atom concentration at the grain boundary can be expressed as:

$$\delta\frac{\partial C_{gb}}{\partial t} = \delta\frac{1}{r}\frac{\partial}{\partial r}\left(D_{gb}^{eff} r \frac{\partial C_{gb}}{\partial r}\right) - 2D_v^{eff}\left(\frac{\partial C_v}{\partial R}\right)_{R=a} \tag{2}$$

subject to the initial condition of $C_{gb}(r,0) = 0$, and the boundary conditions of $C_{gb}(0,t) =$ finite and $C_{gb}(s,t) = 0$. In Eq. (2), C_{gb} is the fission gas concentration at the grain boundary, δ is the grain boundary thickness, and s is the equivalent radius of the grain surface (Fig. 3(b)). This equation must be solved using cylindrical geometry because the solute atom transport process in the grain boundary is basically a surface diffusion from the center of the grain surface to the edge, as seen in Fig. 3. In this formulation, the unique solute atom supply to the grain boundary is the gas atoms arriving at the two adjacent boundaries that face each other. This is the reason that the last term in the RHS is doubled.

Fig. 3(b) shows the concentration balance of the fission gas atoms in the grain boundary. As there is no sudden accumulation or depletion of fission gas atoms at the boundary during steady state operation, mathematical manipulation turns Eq. (2) into the following third kind of boundary condition without any significant loss of analytical foundation [19]:

$$\alpha\left.\frac{\partial C_v}{\partial R}\right|_{R=a} - C_v(a,t) = 0, \tag{3}$$

where $\alpha = \frac{2}{\delta\beta_1^2}\frac{D_v^{eff}}{D_{gb}^{eff}}$.

Then, the short-time approximate solution of the fission gas concentration and the definition of the fractional release yield the fission gas release fraction in the following form:

$$F \cong \frac{4}{\sqrt{\pi}}\left(\frac{a}{\alpha+a}\right)^2\left(\frac{D_v^{eff}t}{a^2}\right)^{1/2} - \frac{3}{2}\left(\frac{a}{\alpha+a}\right)\left(\frac{D_v^{eff}t}{a^2}\right). \tag{4}$$

As can be seen in Eq. (4), multiples of $a/\alpha + a$ appear in each term of the simple Booth solution, factorizing it with a new dimensionless parameter. This result clearly shows that this two-stage model reduces to the simple Booth single stage model when $\alpha = 0$, i.e. the grain surface acts as a perfect sink or when grain boundary diffusivity is infinite. The equation shows that the two competing physical quantities, the equivalent grain radius, a, and the diffusivities ratio, α, seem to determine the role and the effect of the grain boundaries on the release of fission gas atoms. In fact, the term a is not just a radius, but can be interpreted as a volume-to-surface ratio, whereas α can be regarded as a volume-to-surface diffusion ratio. Unless major grain growth occurs during reactor operation, the volume-to-surface ratio is a geometric constant, typically 5–10 μm. On the other hand, the ratio of the grain lattice to the grain boundary diffusion, α, is a variable transport property,

which is strongly dependent on the diffusing fission gas species, the fuel temperature, and the fuel burn-up.

2.2. Two-step two-stage model

Successful depiction of high burn-up fission gas release with the previous model has led to the development of current two-step two-stage model.

As δ is of the order of 10^{-8} cm and β_1 is $2.405/s$ where s is the equivalent radius of the grain surface which is of the order of 10^{-4} cm, the value of $2/\delta\beta_1^2$ is close to unity. Thus, the ratio of diffusivities, α, can be simply reduced in the following way:

$$\alpha \cong \frac{D_{\mathrm{v}}^{\mathrm{eff}}}{D_{\mathrm{gb}}^{\mathrm{eff}}} = \frac{D_{\mathrm{v0}}\mathrm{e}^{-Q_{\mathrm{v}}/RT}}{D_{\mathrm{gb0}}\mathrm{e}^{-Q_{\mathrm{gb}}/RT}}$$

which can be rewritten as

$$\alpha = \alpha_0 \mathrm{e}^{-(Q_{\mathrm{v}},-Q_{\mathrm{gb}})/RT} = \alpha_0 \mathrm{e}^{-Q_{\mathrm{v}}(1-Q_{\mathrm{gb}}/Q_{\mathrm{v}})/RT}, \quad (5)$$

where $\alpha_0 = D_{\mathrm{v}_0}/D_{\mathrm{gbo}}$.

Now burn-up factor, defined as $f_{\mathrm{Bu}} = 1 - Q_{\mathrm{gb}}/Q_{\mathrm{v}}$, is introduced into Eq. (5) in the following way:

$$\alpha = \alpha_0 \mathrm{e}^{-f_{\mathrm{Bu}}Q_{\mathrm{v}}/RT}. \quad (6)$$

Then, the fractional release of fission gas atoms is finally obtained as:

$$F \cong \frac{4}{\sqrt{\pi}}\left(\frac{1}{1+\alpha'\mathrm{e}^{-f_{\mathrm{Bu}}Q_{\mathrm{v}}/RT}}\right)^2 \left\{\left(\frac{D_0}{a^2}\right)\exp\left(\frac{-Q_{\mathrm{v}}}{RT}\right)t\right\}^{\frac{1}{2}}, \quad (7)$$

where $\alpha' = \alpha_0/a$.

In the low burn-up regime, it is believed that fission gas atoms, having diffused through the grain lattice with an activation energy, Q_{v}, surface-diffuse at the grain boundaries with another activation energy, Q_{gb}, while some of these atoms become trapped by the inter-granular bubbles grown at the boundaries. This trapping suppresses the release of the fission gas atoms into the open space in a fuel rod. On the other hand, in the high burn-up regime, especially when it exceeds a threshold burn-up, the inter-linkage of the bubbles begins to remove the barrier for grain boundary diffusion. That is, it lowers the activation energy, Q_{gb}, effectively, and this leads to an enhancement of the grain boundary diffusivity.

In this way, more bubbles interlink, and this increases the number of inter-linkages connected to an open space, so more trapped atoms are released free. Therefore, in the current model, the burn-up factor, f_{Bu}, is treated in a step-wise manner, depending on the fuel burn-up value. The factor is assumed to remain zero until the fuel burn-up reaches a threshold burn-up value because Q_{gb} stays close to Q_{v}. On the other hand, once it exceeds the threshold the factor is presumed to increase linearly up to a value of unity in the high burn-up regime. Ultimate burn-up where the grain boundary diffusion becomes non-activated with the activation energy of zero, i.e. $f_{\mathrm{Bu}} = 1$, is determined from high burn-up in-pile data.

3. Model validation and discussion

In order to derive the constituent parameters and to validate the current model, in-pile measurement data sets available in the FRAPCON-3 code are used [21]. To avoid any unnecessary errors or deviation, all 10 data sets and their input instructions distributed by the FRAPCON-3 code authority are chosen for the derivation, which cover the entire burn-up range, up to about 75000 MWd/MTU.

For the best-curve fitting analysis, 25000 MWd/MTU is taken to be the threshold burn-up value, as recommended by the modified ANS 5.4 model, as well as demonstrated by the recent in-pile data (Fig. 4). The fitting analysis with numerous iterations puts out the following best-fit parameters:

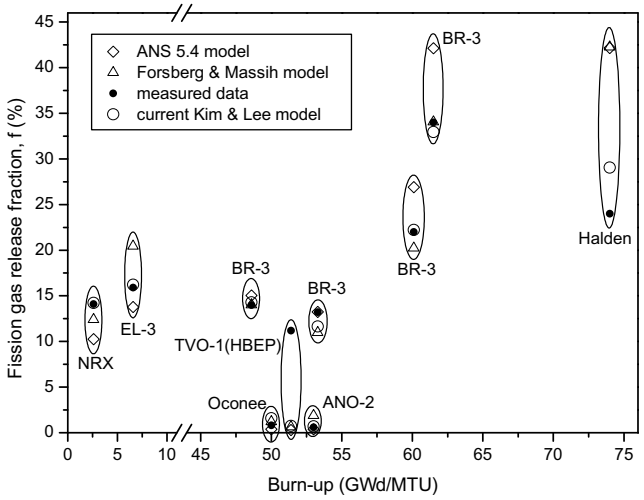

Fig. 5. A comparison of the model predictions with the in-pile measurement data.

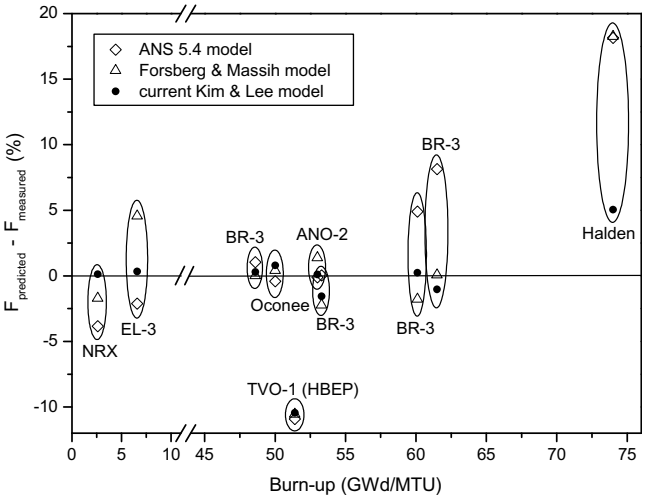

Fig. 6. A plot of the difference between the model predictions and the measurements.

Table 1
A comparison of the constituent model parameters

FGR models	Activation energy, Q_v (kJ/mol)	D_0/a^2 (s^{-1})	Burn-up factor	Resolution, parameter $b\lambda$
ANS 5.4	302.94	0.61	$100^{Bu/28\,000}$	*N/A*
Modified ANS 5.4	208.24	22.1×10^{-4}	$100^{Max(Bu-25\,000)/21\,000}$	*N/A*
Forsberg–Massih	190.52	8.56×10^{-3}	*N/A*	1.84×10^{-14}
Modified Forsberg–Massih	241.94	8.56×10^{-3}	$100^{Max(Bu-21\,000)/35\,000}$	1.47×10^{-12}
Two-step two-stage model	188.16	0.018	$\left[\frac{1}{1+\alpha' e^{-f_{Bu}Q_v/RT}}\right]^2$ where, α'=1.06, $f_{Bu}=Max(0,Bu-25000)/72000$	*N/A*

$\alpha' = 1.06,$

$f_{Bu} = \mathrm{Max}(0, \mathrm{Bu} - 25000)/72000,$

$(D_0/a^2) = 0.018/\mathrm{s},$ and

$Q_v = 188.16\ \mathrm{kJ/mol}.$

Using these derived parameters, model predictions are checked against the data sets again and compared with other popular model predictions. As shown in Fig. 5, the predictions are in much better agreement with the measurements than those of any other models built in the code, such as ANS 5.4, modified ANS 5.4, and Forsberg–Massih models over the entire burn-up range up to about 75000 MWd/MTU. A plot of the difference between the predicted and the measured values is shown in Fig. 6, which clearly demonstrates that current Kim and Lee model predicts the release fractions most closely towards the in-pile measurement data.

It is noticeable that other model predictions significantly deviate from the measurements with increasing fuel burn-up except current model. This can be easily understood when we review the burn-up factors of the models. The factor of current model is mechanistically derived and thus saturates to unity as the fuel burn-up increases. However, the others increase just exponentially as the burn-up goes up, which is incorrect.

The TVO-1 measurement data, as commonly pointed out by many colleagues, seems to be extraordinarily high compared to the reported power profile during the in-pile experiment. All the mechanistic models, including current model, predict much lower release fraction than the measured one.

Table 1 lists the constituent parameters of the models for the comparison, which shows that the parameters of current Kim and Lee model are in similar ranges to those of the other popular models. In particular, the activation energy of the effective diffusion coefficient is close to those of the modified ANS 5.4 model and original Forsberg and Massih model. Through the best-curve fitting analysis the ultimate burn-up is determined to be 97000 MWd/MTU.

4. Conclusions

Based on the recent theoretical model, a two-step two-stage model is developed with the incorporation of a step-wise burn-up factor. This factor is derived with the assumption that the activation energy of grain boundary diffusion is identical to that of grain lattice diffusion in the low burn-up regime, whereas it begins to decrease linearly down to zero in the high burn-up regime once the fuel burn-up exceeds a threshold burn-up. This threshold value is set to be 25000 MWd/MTU as recommended by the modified ANS 5.4 model and demonstrated by compiled in-pile data. In the mean time, the ultimate fuel burn-up at which the grain boundary diffusion becomes non-activated with zero activation energy is derived to be 97000 MWd/MTU through best-curve fitting analysis.

FRAPCON-3 code and its in-pile measurement data sets are used to derive the constituent parameters and to validate the model. Results show that, over the entire burn-up range up to 75000 MWd/MTU, current model predictions are in better agreement with the measurements than those by any other models built in the code, such as ANS 5.4, modified ANS 5.4, and Forsberg–Massih models.

The outstanding agreement supports that this two-step two-stage approach formulated in this study seems to be founded on a sound mechanistic basis. In actuality, it is noticeable that the introduction of the step-wise burn-up factor in the model successfully separates the burn-up factor from the conventional diffusion coefficient mixed with the empirically derived burn-up enhancement factor.

A comparison of the constituent parameters of the models shows that current Kim and Lee model can go well with the built-in models in the FRAPCON-3 code. In particular, the activation energy of the effective diffusion coefficient turns out to be close to those of the modified ANS 5.4 model and original Forsberg and Massih model.

Acknowledgement

This work was partially supported by the research fund of Hanyang University (HY-2005-I), Seoul, Korea.

References

[1] R. Manzel, M. Coquerelle, in: Proc. ANS Int. Topical Meeting on LWR Fuel Performance, Portland, Oregon, USA, March 2–6, 1997, p. 463.
[2] J.O. Barher, M.E. Cunningham, M.D. Freshley, D.D. Lanning, Nucl. Tech. 102 (1993) 210.
[3] K. Une, K. Nogita, S. Kashibe, M. Imamura, J. Nucl. Mater. 188 (1992) 65.
[4] C.C. Dollins, M. Jursich, J. Nucl. Mater. 105 (1982) 269.

[5] S. Bremier, C.T. Walker, R. Manzel, in: Proc. Int. Seminar on Fission Gas Behavior in Water Reactor Fuels, Cadarache, France, September 26–29, 2000.
[6] M. Tourasse, M. Boidron, B. Pasquet, J. Nucl. Mater 188 (1992) 49.
[7] M.E. Cunningham, M.D. Freshley, D.D. Lanning, J. Nucl. Mater. 200 (1993) 24.
[8] D.R. Olander, P. Van Uffelen, J. Nucl. Mater. 288 (2001) 137.
[9] F. Lemoine, J. Papin, J.M. Frizonnet, B. Cuzalis, H. Rigot, in: Proc. Int. Seminar on Fission Gas Behavior in Water Reactor Fuels, Cadarache, France, September 26–29, 2000.
[10] M. Paraschiv, A. Paraschiv, J. Nucl. Mater. 185 (1991) 182.
[11] D.R. Olander, in: I.J. Hastings (Ed.), Advances in Ceramics, vol. 17, The American Ceramic Society, Columbus, Ohio, 1986, p. 271.
[12] M.V. Speight, J.A. Turnbull, J. Nucl. Mater. 68 (1977) 244.
[13] J.A. Turnbull, C.A. Friskney, J. Nucl. Mater. 58 (1975) 31.
[14] A.H. Booth, AECL Report CRDC-721, 1957.
[15] M.V. Speight, Nucl. Sci. Eng. 37 (1969) 180.
[16] J.A. Turnbull, J. Nucl. Mater. 50 (1974) 62.
[17] R.J. White, M.O. Tucker, J. Nucl. Mater. 113 (1983) 1.
[18] K. Forsberg, A.R. Massih, J. Nucl. Mater. 127 (1985) 141.
[19] Y. Kim, J. Nucl. Mater. 326 (2004) 97.
[20] Y. Hirano, Y. Mozumi, K. Kamimura, Y. Tsukuda, in: Proc. ANS Int. Topical Meeting on LWR Fuel Performance, Kyoto, Japan, October 2–6, 2005, p. 403.
[21] NUREG/CR-6534, PNNL-11513, 1997.